A PHYSICAL STEADY-STATE PERFORMANCE MODEL FOR MIXED EXHAUST SYSTEMS OF TURBOFAN ENGINES

J. Wachter

EE-1, Performance & Analysis
Rolls-Royce Deutschland Ltd. & Co KG
Eschenweg 11
15827 Blankenfelde-Mahlow

S. Staudacher

Institut für Luftfahrtantriebe
Pfaffenwaldring 6
70569 Stuttgart

Abstract

Mixed exhaust systems offer potentials to improve gross thrust performance and noise emission patterns of turbofan engines. However, steady-state modelling within engine performance simulations is challenging because of the highly three-dimensional flow induced by vortices that are generated e.g. by the forced mixing device. Approaches to model these effects in great detail often reduce the fidelity of the performance model. They can hardly be covered by general one-dimensional meanline approaches.
This paper introduces a strictly physical model for mixed exhaust configurations. It is set up by means of modelling the dominating effects occurring in the defined control volume. It will be shown, that this approach is suitable to be matched against rig-test results as well as against engine test data successfully. The necessary changes of matching constraints for the usage within performance synthesis models is discussed and the advantages against conventional modelling approaches are pointed out by a representative case study.

1. NOMENCLATURE

A	Area
CD	Discharge Coefficient
CF	Thrust Coefficient
$CEPR$	Cold Exhaust Pressure Ratio
CP_9	Nozzle Exit Pressure Factor
DPP	Total Pressure Loss
EPS	Exhaust Pressure Split
ETR	Exhaust Temperature Ratio
F_g	Gross Thrust
k_s	Wall roughness coefficient
$\dot{m}$	Discharge
N	Limited Pressure Ratio
P	Total Pressure
p	Static Pressure
Q	Discharge Function
R	Specific Gas Constant
Re	Reynolds Number
SFC	Specific Fuel Consumption
T	Total Temperature
t	Static Temperature
u	Velocity
Δ	Nozzle Exit Profile Elevation
κ	Adiabatic Coefficient
ρ	Density
η_{mix}	Mixing efficiency
ζ	Non-Dimensional Radius

2. INTRODUCTION

The relevance of exhaust subsystem modelling is mainly driven by its high influence on the overall performance of a turbofan engine. Especially the level of the fan working line, gross thrust and hence the specific fuel consumption are directly impacted by the quality of exhaust models. It is vital for on- as well as for off-design calculations that those overall engine characteristics are known with high precision to ensure for instance optimum fan efficiency, at least the required stability margin and achievement of specified SFC guarantees.
This paper contributes to an improved understanding of the physical performance of a forced mixer exhaust system and its influence on overall engine parameter by means of introducing an extended modelling approach. It will be demonstrated, that physical effects emerging in this component are accounted for and thus lead to an improvement in engine performance simulations.
Moreover it provides incitations to modelling challenges of other mixing related applications, like for instance the insertion of cooling flows into gas paths.

3. EXHAUST MODELING PHILOSPHIES

In performance programs the component module of a mixed exhaust system typically comprises the control volume as generically sketched in Figure 1.

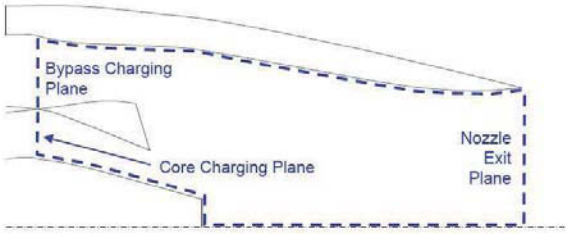

Figure 1: Control Volume of a mixed exhaust system

Its entry planes are defined at hardware interface of the mixing device to the core fairings for the hot core and cold bypass duct respectively. The control volume exit shall be defined at the nozzle exit plane. All thermo- and gasdynamic effects occurring within that control volume need to be reflected by the respective performance model.

First approaches on that subject are discussed in literature since the 1960s. Performance assessments were conducted for instance by Frost [1] and Pearson [2] to conclude on the impact of engine cycles. They applied so-called *one-stream models*, which accounts for full mixing of the hot core and the cold bypass gas in the exhaust system. Those calculations are introduced generally as an ideal process, hence allow for the conservation of system energy, mass-momentum and discharge flow during the mixing calculation. Those models can be used to quantify the thermodynamic gain of mixed exhaust systems relative to separate jet exhaust configurations. However they do not account for side effects like additional losses, e.g. caused by complex mixer geometries, free shear layers, vortices and partial mixing.

Such effects were accounted by a new modelling approach as discussed by Alexiou [3] and Köhli [4]. Similar as depicted above an ideal mixing calculation is processed in this model, however only for a predefined fraction. The remaining flow portions are passed through the exhaust volume without changing their thermodynamic states. As this model accounts for three individual streams in the nozzle exit plane it shall be denoted as *three-stream model*. The quantification of the performance in terms of fractional mixing might be expressed as quoted in [5] by the parameter *mixing efficiency* $\eta_{mix,3\text{-stream}}$

$$\eta_{mix,3-stream} = \frac{\dot{m}_{mixed}}{\dot{m}_{cold,charging} + \dot{m}_{hot,charging}}. \quad (1)$$

Physical effects are taken into account with much more detail than in the one-stream models, as real nozzles also show “varying degrees of radial temperature profiles with regions of hot core flow that were not effectively mixed with the fan stream” [6]. However, mixing efficiency merely defines a performance measure and does not claim to represent the real physical temperature distribution. Furthermore, the split up of the two incoming streams into a third one comes along with a loss of accuracy in terms of performance modelling parameter as discussed in [7]. This is mainly reasoned by the necessary back-to-back testing in order to establish modelling coefficients for the three-stream model. The raised uncertainty adversely impacts performance synthesis results as fan working line levels as well as specific fuel consumptions.

The three-stream model generally accounts for parasitic effects with two primary nozzle coefficients, the *discharge coefficient*

$$CD = \frac{\sum_{i=\{cold,mixed,hot\}} A_{eff,i}}{A_{geo,throat}} \quad (2)$$

and the *thrust coefficient*

$$CF = \frac{F_{g,real}}{\sum_{i=\{cold,mixed,hot\}} \dot{m}_i \, u_{i,ideal}}. \quad (3)$$

Those performance parameter are usually fed into the model as characteristics based on the non-dimensional operating condition of the exhaust system, which is described by the two pressure ratios,

cold exhaust pressure ratio

$$CEPR = \frac{P_{bypass,charging}}{p_{\infty}} \quad (4)$$

and *exhaust pressure split*

$$EPS = \frac{P_{bypass,charging}}{P_{core,charging}}. \quad (5)$$

With the assumption of an unchoked operating condition of the nozzle, the thrust equates to

$$F_{g,real} = CF \sum_{i=\{cold,mixed,hot\}} \dot{m}_i \, u_{i,ideal} \quad (6)$$

and the discharge will be limited by the effective throat area

$$\sum_{i=\{cold,mixed,hot\}} A_{eff,i} = CD \; A_{exit,geo}. \quad (7)$$

A special breakdown of this three-stream-approach is established with the definition of zero mixing, which is denoted as *two-stream model*. This method results in the complete, separate conservation of the thermodynamic states of the entering massflows. To account for the apparent physical effects, it is necessary to extend the non-dimensional groups of the nozzle operating condition by introducing the *exhaust temperature ratio*

$$ETR = \frac{T_{core,charging}}{T_{bypass,charging}} \quad (8)$$

in order to cover thrust augmentation as well as thermal throttling due to the hot/cold mixing effect [8]. The second main difference to the three-stream model sets the split up of the discharge coefficient CD (see equation (2)),

which is not applicable for two-stream methods anymore. Instead of, the two separate effective nozzle throat areas $A_{eff,hot}$ and $A_{eff,cold}$ are defined separately as function of the extended operating condition as defined in equations (4), (5) and (8). Effective areas are defined as

$$A_{eff} = \frac{\dot{m}\sqrt{T}}{P\,Q}, \tag{9}$$

where Q is the discharge function

$$Q = \sqrt{\frac{2\,\kappa}{(\kappa-1)\,R} N^{\frac{-1-\kappa}{\kappa}} \left(N^{\frac{\kappa-1}{\kappa}} - 1 \right)} \tag{10}$$

and N the pressure ratio over the nozzle duct, with an upper limit set by the critical pressure ratio

$$N = \begin{cases} P/p_{\infty} & for\ P/p_{\infty} < P/p_{crit} \\ P/p_{crit} & for\ P/p_{\infty} \geq P/p_{crit} \end{cases}. \tag{11}$$

As third coefficient the thrust coefficient remains unchanged to the one depicted for the three-stream-model and defined in equation (3).
Compared to the three-stream-method this approach goes along with the advantage, that it can be directly used to analyse rig-test data as its performance parameters are solely dependent on pure measurement data. It could be shown in [7], that this fact improves model accuracy against other modelling philosophies although physical effects are comprised in overall system coefficients.

A brief comparison of the most important differences of the stated performance models is provided with Table 1.

	1-Stream-Models	**2-Stream-Models**	**3-Sream-Models**
Existence of mixed Stream	Yes: 100% of entering flow discharges	No	Yes: Partially mixed entering flow discharges
Physical Represen-tation	Low: Full mixing is never observed	Low: Zero mixing is never observed	Medium: Partial mixing resembles reality not perfectly
Model Para-meters	Discharge- & Thrust Coefficient	Effective Throat Areas & Thrust Coefficient	Mixing Efficiency, Discharge- and Thrust Coefficient
Accuracy of Para-meters	High: Robust modelling approach	High: Robust modelling approach	Low: Back-to-Back testing necessary

Table 1: Mixed Exhaust System Model Comparison

4. EXTENDED APPROACH

To cope with the mentioned modelling shortfalls, a strictly physical approach shall be baseline for the generation of an advanced steady-state exhaust performance model. It shall combine the advantages of a two-stream model with a full physical representation the gas- and thermodynamic effects occurring in the exhaust system. The first step for this task is the identification of the most important individual flow effects, emerging in the control volume.

4.1. Elementary Flow Models

A detailed analysis of rig-test data and comparable CFD studies concluded in four main contributors for observable gasdynamic effects in the main gas path.

- *Wall friction* is induced by the mixing device, the bullet and the inner jet pipe surface. Friction forces can be approximated by application of pipe friction calculation [13].
- The *mixing* process of gas jets causes pressure losses, which can be quantified as shown by Oates [8].
- Besides the pure mixing, *heat is transferred* in the mixing chamber from the hot core flow to the cold bypass jet and thus augments the exhaust system performance [10].
- Finally, *expansion* of the flow from the charging stations to ambient atmosphere is an obvious effect in the exhaust system [14].

Those four items are labelled as “elementary flow models” within this paper and baseline for the generation of a physical description of a mixed exhaust system.

4.2. Gross Thrust calculation

The gross thrust of the turbofan engine shall be solely computed by the exhaust performance parameters and is driven by

- the exiting momentum of the discharge and
- static pressure differences, emerging from eventual over- or underexpansion of the exiting flow of the nozzle.

The resulting, ideal gross of the exhaust performance model is shown by equation (12)

$$F_g = \sum_{i=\{hot,cold\}} \dot{m}_i\, u_i + A_{exit}\left(p_9 - p_{\infty}\right). \tag{12}$$

4.3. Segmentation of the Control Volume

To allow proper classification of individual physical effects, the overall control volume as outlined in Figure 1 is split into several control volumes. Figure 2 shows the respective subvolumes and nomenclature of the discussed exhaust model.

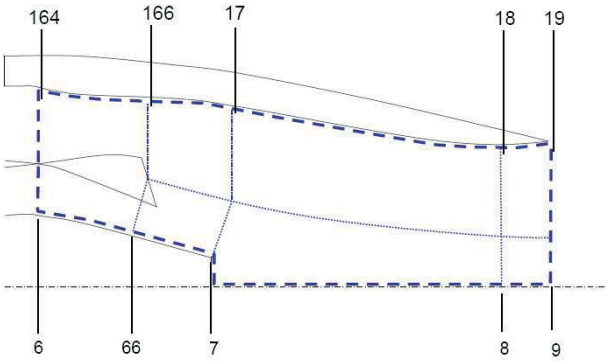

Figure 2: Model Nomenclature

The entering cold and hot flow is passed through a mixer section, which begins at the upfront end of the mixing device (6 & 164) and ends at the virtual plane, representing the downstream end of the mixer chutes (66 & 166). Mixing related calculations are processed as next step. This subvolume shall end at the bullet trailing edge (7 & 17). The convergent duct of the nozzle, which is the main contributor to the acceleration of the exhaust flow discharge follows to this subsection. Its downstream boundary plane is set at the nozzle throat (8 & 18).
For convergent-divergent nozzles the final subvolume is the diverging part, ending with the nozzle exit plane (9 & 19). The separate modelling of the convergent part is of significant importance as losses occurring in this portion do not impact the discharge throttling of the throat area anymore.

This model approach is to be classified as a two-stream model as introduced in chapter 3. There is no physical mixture of discharges allowed in the entire control volume. Furthermore, static pressure balance between hot and cold flow is ensured for all downstream positions from 66 and 166 onwards. This postulation was judged to be applicable for the common operating condition of an exhaust system, although it is claimed in the literature, that the pressure balance flaws for regimes with very high pressure splits as they might occur at subidle cruise conditions [11]. However, these power conditions shall not be subject of this steady-state model setup.

4.4. Assignation of Elementary Flows

The elementary flows as discussed in section 4.1 are now assigned to the individual sub control volumes. Not every elementary flow model is applicable to each sub volume. The assignment currently used is as denoted in Figure 3.

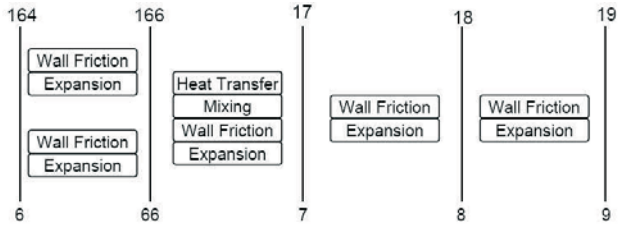

Figure 3: Assignation of elementary flow models

Wall friction and expansion are assumed to occur in all non-constant area ducts. Forced mixing and heat transfer are only accounted in the mixing zone sub volume. This approach is based on the assumption that no mixing occurs in the nozzle portion, which clearly simplifies the physics in real exhaust systems. However, it will be demonstrated, that this assumption allows a proper accounting of the mixing effects without negative impact on the model applicability.

4.5. Performance Coefficients

As the physical exhaust system only accounts for ideal thermo- and gasdynamic processes so far, performance coefficients need to be established, which constitute the actual performance of a design status. Following subsections discuss the different parameters, which are introduced for this performance model.

4.5.1. Wall smoothness

All control volumes are affected by wall friction due to the mixer chute, bullet and inner nozzle duct surfaces. In order to calculate the friction forces, the wall roughness coefficient k_s needs to be known as discussed in [13]. This parameter and the respective wetted areas are specified per user input into the model.

4.5.2. Partial Entropy raise due to Mixing

One of the intentions of the mixing zone in the model is to derive the potential entropy raise for a fully mixed system, which is associated with a thermodynamic mixing process. This entropy raise leads to a total pressure loss over the mixing zone, which will only be partially observable since mixing is not fully performed in reality. To account for this mismatch, a mixing coefficient $\eta_{mix,m}$ is introduced, which adjusts the maximum theoretical pressure loss to an observed value.

(13) $$P_{7/17} = P_{66/166}\left(1-\eta_{mix,m}\ DPP_{mix,\max}\right), \text{ with}$$

(14) $$DPP_{mix,\max} = 1-\frac{\dot{m}_{66}\ P_{66}+\dot{m}_{166}\ P_{166}}{\left(\dot{m}_{66}+\dot{m}_{166}\right)P_{966,virt}}.$$

The newly introduced state $P_{966,virt}$ is meant to be a total head pressure, which would be computed by a full mixing of the entering streams. This is calculated only for the derivation the total pressure loss *DPP* in the elementary flow model and is not used as thermodynamic state in the exhaust model.

4.5.3. Partial Heat Transfer

The same rationales as discussed in paragraph 4.5.2 apply to the modelling of the heat transfer between hot and cold stream in the mixing zone. Hence, a second mixing performance coefficient is defined, which controls the amount of actual transferred heat by a coefficient $\eta_{mix,T}$. This parameter directly influences the driving physical effect of the heat transfer, the static temperature difference between the bypass and core flow

(15) $$\eta_{mix,T} = 1-\frac{t_7-t_{17}}{t_7^*-t_{17}^*}.$$

Temperatures, marked with an asterisk are defined to be reference static temperatures, which are derived by applying no heat transfer at all. Thus, their difference equals the maximum possible temperature offset of the modelled hot core to the cold bypass stream

4.5.4. Accounting of pressure and temperature profiling at the nozzle exit plane

Per definition the one-dimensional model allows for mean values in the exhaust model only. It is assumed that the model contains the information of the mass-weighted thermodynamic states in the respective performance planes. However the nozzle exit pressure also need to be available in the form of an area-weighted scalar as this drives the force, which needs to be applied in the pressure term of equation (12). This is demonstrated by expanding the pressure term into an area integral

$$(16)\quad A_{exit}\left(p_9 - p_\infty\right) = \iint_{r,\varphi} r\left[p_9(r,\varphi) - p_\infty\right] dr\, d\varphi\,.$$

This proves the necessity to compute area-weighted, static nozzle exit pressures as defined in equation (17)

$$(17)\quad p_{9,a-w} = \frac{\iint r\; p_9(r,\varphi)\, dr\; d\varphi}{A_{exit}}\,.$$

The model copes with this requirement by provision of a factor CP_9 on the modelled mass-weighted static exit pressure in order to derive the area-weighted value

$$(18)\quad p_{9,a-w} = p_{9,m-w}\, CP_9\,.$$

Further numerical investigations have indicated, that pressure as well as temperature patterns at the nozzle exit plane can be well approximated by parabolic profiles. Hence, the pressure distribution may be written as function based on the wall parameters $p_{9,wall}$ and $t_{9,wall}$ by

$$(19)\quad p_9(\varsigma) = p_{9,wall}\left(1 + \Delta_p - \Delta_p\, \varsigma^2\right) \text{ and}$$

$$(20)\quad t_9(\varsigma) = t_{9,wall}\left(1 + \Delta_T - \Delta_T\, \varsigma^2\right),$$

where the introduced parameters Δ_P and Δ_T represent the maximum pressure and temperature elevation respectively. The radial coordinate r is corrected by $\varsigma = r / R_{nozzle\ exit}$ for simplification purposes.

Figure 4 illustrates exemplarily such a profile as derived by CFD assessments. This profile is representative for a choked throat condition at a nozzle pressure ratio of 3,2.

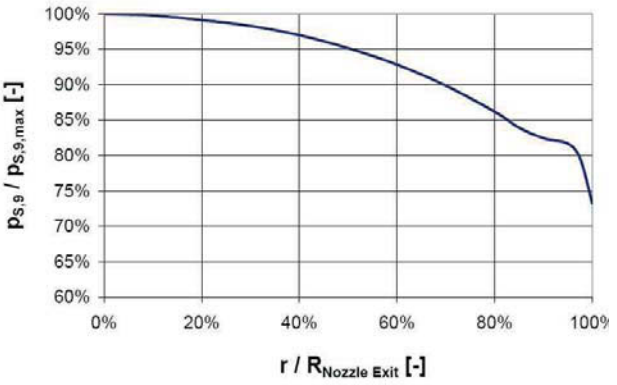

Figure 4: Radial static pressure profile at nozzle exit plane

The performance coefficient CP_9 can directly be evaluated by means of comparison of the averaged values, which are established from the different weighting approaches

$$(21)\quad CP_9 = \frac{\int_{\varsigma=0}^{1} 2\pi\, p(\varsigma)\,\varsigma\, d\varsigma \;\; \int_{\varsigma=0}^{1} 2\pi\, \rho\, u\, \varsigma\, d\varsigma}{\pi \int_{\varsigma=0}^{1} 2\pi\, \rho\, u\, p(\varsigma)\,\varsigma\, d\varsigma}\,.$$

Note, that CP_9 is also to be considered as model input parameter as this parameter is dependent on the exhaust design and impacts directly the calculated gross thrust as shown in the updated equation (22)

$$(22)\quad F_g = \dot{m}_9\, u_9 + \dot{m}_{19}\, u_{19} + A_{exit}\left(CP_9\; p_9 - p_\infty\right).$$

4.5.5. Performance Coefficient Overview

A brief overview of the introduced performance coefficients and their objective in the model is given in Table 2.

Parameter	Accounts for…
k_s	wall roughness losses
$\eta_{mix,m}$	entropy raise due to gas mixing
$\eta_{mix,T}$	entropy raise due to heat transfer
Δ_P	pressure elevation in nozzle exit plane
Δ_T	temperature elevation in nozzle exit plane

Table 2: Model Input Parameters

5. A CALIBRATION AGAINST EXHAUST RIG-TESTS

During the development of a two-shaft turbofan engine at Rolls-Royce Deutschland, performance rig tests of a mixed exhaust system were conducted. Those data were used to perform a model calibration by adjustments of the performance parameters as summarized in Table 2. The

calibration process against these rig-test data and the results are discussed within this paragraph.

5.1. Test strategy of mixed exhaust rig tests

In order to obtain the full performance understanding of a mixed exhaust system it is common practice to conduct testing in three different configurations.

- The first hardware test setup comprises an exhaust system with an annular mixer and ambient core temperature, which sets the exhaust temperature ratio to unity. Intention of this configuration is to evaluate the baseline performance of a reference system without introducing complex physical effects of forced mixing by a lobed mixer design and heat exchange due to a temperature difference between the two entering flow discharges.
- For the second configuration the mixer hardware is exchanged with the final design standard but the cold core stream is retained. This allows for the identification of the additional losses due to the complex, lobed mixer geometry. Beneficial mixing effects, which are driven by raising the temperature ratio between the jets [8] do not influence this part test.
- A final configuration is consecutively tested, for which the core temperature is increased on levels as expected for actual engine operation. This finally enables the determination of the mixing benefit of the system end concludes on the overall performance of the exhaust system.

5.2. Calibration of the performance model

The available dataset includes all of the above-mentioned configurations and hence allow the individual determination of the model performance coefficients.

The calibration of the coefficients was done by introduction of the requirement, that the sum of the synthesised hot and cold exhaust throat area is equal to the geometric size of the nozzle throat.

$$(23)\quad A_{8,syn} + A_{18,syn} \overset{!}{=} A_{geo,throat}$$

This postulation is valid as the performance model accounts for all applicable pressure losses upstream of the throat area and reduces charging pressure in plane 8 and 18.

Following paragraphs outline the proposed method for the rig test analysis with the physical exhaust model. Results of an actual calibration process will be presented in section 5.3.

5.2.1. Evaluation of wall roughness parameter

The performance coefficient k_s, reflecting wall roughness quality can be evaluated by analysing data of the forced mixed system with *ETR* = 1,0 and *EPS* = 1,0. This setting induces least influences due to heat transfer and high velocity gradients of the incoming gas jets. Remaining losses of secondary effects like pressure losses generated by shed vortices or shear layer effects are assumed to be negligible in comparison to the wall friction impacts.

5.2.2. Determination of partial entropy raise due to mixing

For the evaluation of the performance coefficient $\eta_{mix,m}$ the full dataset for an *EPR* = 1,0 and various *EPS* ≠ 1,0 are assessed. This configuration addresses all physical effects, which are driven by the raise of viscous effects caused by the freestream shear layer within the mixing zone.

5.2.3. Determination of partial heat transfer

Rig tests carried out with a provision of hot core flow facilitate the derivation of the partial heat transfer coefficient $\eta_{mix,T}$. This configuration includes the full thermodynamic behaviour of a mixed exhaust system and therefore enables to finish the thermodynamic calibration of the performance model.

5.2.4. Pressure and Temperature Elevation at nozzle exit plane

As discussed in section 4.5.4, pressure and temperature profiles in the nozzle exit planes need to be accounted in the performance model to enable a proper evaluation of the thrust equation (12). This is the only performance parameter, which is solely based on numerical studies since the calibration task as the rig test did not comprise traversing of the exit plane.
Assessments of CFD studies, which were conducted internally at Rolls-Royce Deutschland in parallel to rig-testing, concluded in a quantification of the profile raise parameter Δ_P. It shall be postulated without further proof that Δ_P can be linearly correlated to the Reynolds-Number in the nozzle exit plane

$$(24)\quad \Delta_P = \frac{\mathrm{Re}_{exit}}{\mathrm{Re}_{datum}}.$$

Although this correlation is judged to be empirical so far and needs further investigations to conclude in physical backgrounds, it describes the observed findings very accurately.

The elevation of the temperature profile can be described in well alignment of the CFD studies by the modelled exit temperatures T_9 and T_{19} with

$$(25)\quad \Delta_T = 0{,}5\,\frac{T_9 - T_{19}}{T_{19}}.$$

It needs to be emphasized, that this performance measures are only influencing the pressure term of the thrust equation (12). Thus, they do not affect the calibration requirement as set with equation (23). However its qualification can be proven by comparing synthesized thrusts with measured ones, which is subject of section 5.3.

5.3. Calibration Results

The model was calibrated according to the outlined process against the results of the rig-test analysis. All model parameters were found to be constant throughout for this purpose. This fact indicates, that the chosen ideal similarity processes are well chosen as the observed reality satisfy them with a constant offset.

To show agreement with the rig-test results, discharge- and thrust coefficients (see equations (2) and (3)) are compared from those of the discussed model with those of the rig-test analysis. As the rig-test was assessed by a two-stream approach, it is denoted as such in Figure 5 and Figure 6.

Furthermore it is demonstrated that the double standard deviation 2s of the difference of both models is well in between a confidence band of ±0,5% (see [9] for further details). This difference is within the expected absolute measurement accuracy for all recorded operating conditions of the rig-test.

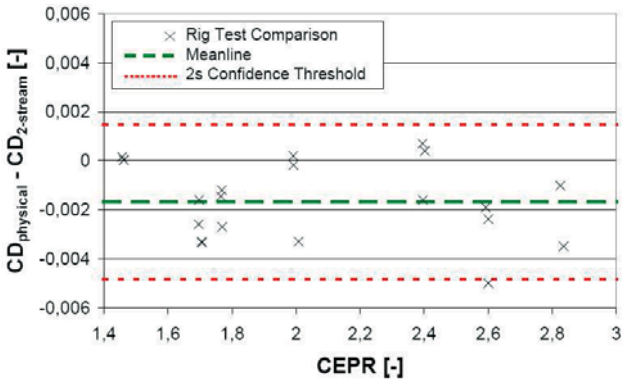

Figure 5: Comparison of Discharge Coefficient

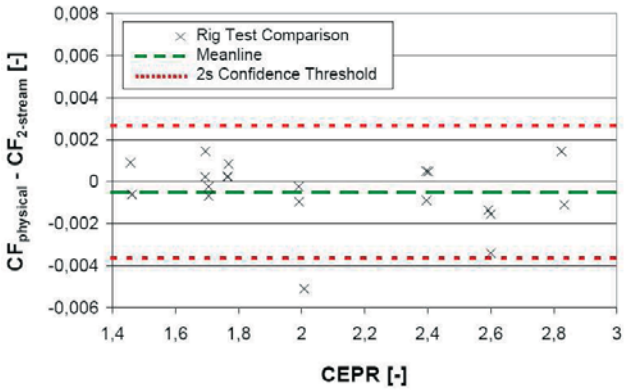

Figure 6: Comparison of Thrust Coefficient

Hence it can be concluded that the herein discussed performance model is capable to achieve full system compliance with the rig-test results by a calibration process as outlined in this section.

5.4. Summary of Calibration Process

It has been shown, that model calibration can be processed with the rig-test strategy as described in section 5.1. This process needs to be based on different rig-test configuration, each applying either different hardware or exhaust system operating condition settings. The performance parameters are therefore matched against the individual part tests and thus can be established individually. Table 3 summarizes the different test configuration and their connection to the performance parameters briefly.

Parameter	CEPR	EPS	ETR	Other
k_s	varied	1,0	1,0	n/a
$\eta_{mix,m}$	varied	varied	1,0	
$\eta_{mix,T}$	varied	varied	varied	
Δ_P	n/a	n/a	n/a	CFD or Traversing
Δ_T				CFD or Traversing

Table 3: Rig-Test Configurations for Model Calibration

6. SYNTHESIS CALCULATIONS

In order to integrate the introduced exhaust model in a full thermodynamic engine model it needs to show compatibility with the adjacent components and the cycle calculation process. This capability is demonstrated within this chapter.

6.1. Performance Model iteration constraints

The implementation of the stand-alone exhaust system model into a full steady-state performance model requires iteration constraints to allow for an iterative cycle calculation. Exhaust models without calculation of mixed streams, need to provide at least two constraints to the cycle matching, to define the limiting areas of both incoming jets. Those constraints need to be established for the discussed modelling approach.

The first choice is trivial in the light of the model calibration as demonstrated in 5.2. The requirement, that the combined, synthesised nozzle throat area equals the geometrical one remains applicable also for the off-design engine cycle calculation as outlined in equation (23).

This formulated constraint will limit the total nozzle exit flow, which is passed through the nozzle duct. However it does not define the portions of the bypass and core flow of this total amount. Thus the second requirement shall be defined as the ratio of the cold to the hot nozzle throat

area, which is set to a fixed ratio, which itself is initially supposed to be a function the operating condition

$$\frac{A_{18,syn}}{A_{8,syn}} = f(operating\ condition)\,. \tag{26}$$

This dependency of the throat area ratio is mandatory to be defined and will be subject to further discussion in further detail in chapter 7.2.

6.2. Performance Model Results

Engine cycle calculations were carried out with a thermodynamic engine simulation program for a mixed two-shaft turbofan engine including the discussed exhaust system model. The advantage of this approach now pays off against conventional modelling approaches as sketched in chapter 3, where the entire physical behaviour is condensed in various performance parameters like discharge- and thrust coefficients.

This fact shall be demonstrated by a case study at a typical cruise operating flight condition for which the parasitic and beneficial effects occurring in the control volume of the exhaust system are clearly separated. Figure 7 shows therefore a performance waterfall chart for the ideal gross thrust the system is capable to generated at the various system calculation steps.

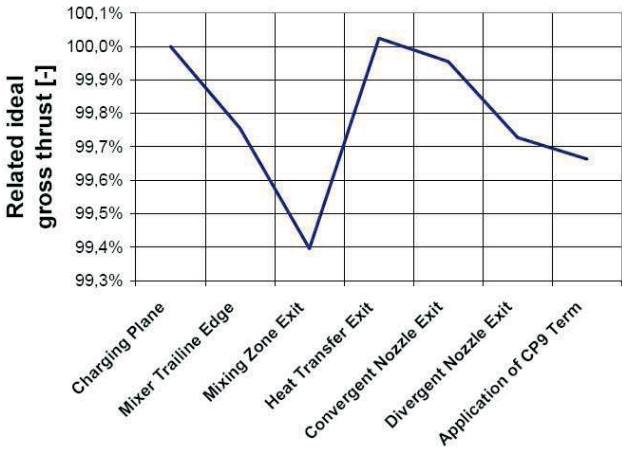

Figure 7: Gross Thrust Waterfall Chart

The thrust decreases continuously with proceeding through the exhaust system with the exception of the mixing zone. This step introduces the thermodynamic mixing gain into the cycle per heat transfer. In Figure 8, the different losses are broken down into a pie chart in terms of total pressure losses. This plot clearly indicates the main contributors to the performance penalties of the system and is hence an expedient indicator for further optimisation of this engine component.

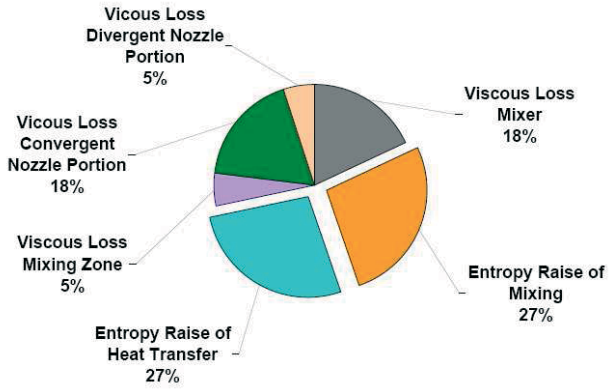

Figure 8: Parasitic Performance Loss Fractions

It worthwhile to mention, that the gain in gross thrust through the mixing zone is now oppositional shown as a major contributor to the total pressure loss. This is due to the inherent nature of the irreversible heat transfer to raise the entropy of the system. However the overall change of the individual enthalpy fluxes in the system cause this process to improve engine cycles in terms of thrust yield as seen in Figure 7.

7. VALIDATION WITH ENGINE TESTS

7.1. Calibration against turbofan engine testing

An engine test series with turbofan engines was used to gain a better understanding for the usage of the model for ANSYN analysis [12]. The engines were configured with an instrumentation standard, which allows for thrust measurement, the recording of charging pressures and temperatures as well as discharge flows. Thus, a direct comparison between the whole engine analysis and rig-test results is valid from a measurement system point of view.

A comparison of modelled and measured gross thrust is shown in Figure 9. Only slight modifications on the input parameter became necessary in order to match the engine cycle. Those rely on hardware non-conformances, of the development hardware. However the capability of the integration into a full thermodynamic engine model makes it suitable for advanced analysis methods, like the ANSYN approach.

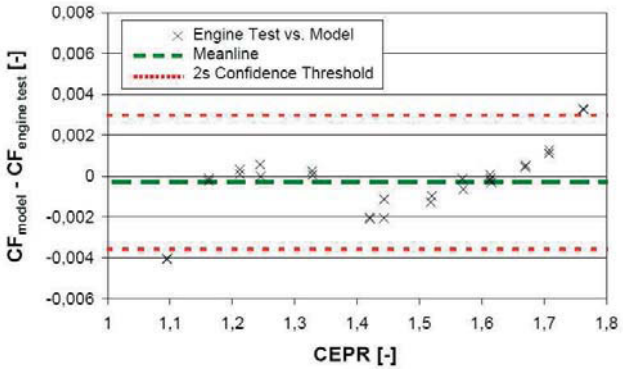

Figure 9: Calibration of physical exhaust model against sealevel engine testing

Again levels of doubled standard deviations are shown, which are sensible smaller than rig-test accuracies and acceptance levels of steady-state performance models. This finding finally provides evidence of the practical applicability and fidelity of the introduced modelling approach and outlines itself with the advantages discussed in section 6.2 to other mixed exhaust modelling philosophies.

7.2. Performance impact of changing nozzle sizes

A further test series was carried out with different nozzle sizes. The fitted nozzle sizes cover a range from -4% to +4% against a nominal nozzle throat area and are shown in Table 4.

Curve	A	B	C	D	E
Nozzle Size	-4% to datum	-2% to datum	Datum size	+2% to datum	+4% to datum

Table 4: Nozzle Area Sizes

Some analysis results are shown in Figure 10. It becomes obvious, that the matching constraint as depicted in equation (26) is in very good agreement with the discharge ratio of the entering massflows. Thus it can be substantiated.

$$(27)\quad \frac{A_{18,syn}}{A_{8,syn}} = f\left(\frac{\dot{m}_{164}}{\dot{m}_6}\right).$$

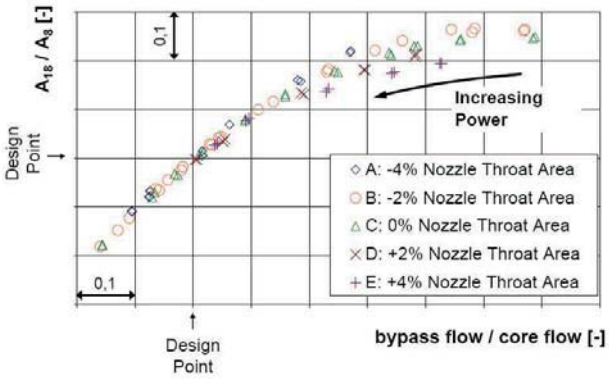

Figure 10: Nozzle Variation Test

The correlation between the measures $A_{18,syn} / A_{8,syn}$ and $\dot{m}_{164} / \dot{m}_6$ seems not to be surprising as it is expected, that the virtual separation streamline is moving to the centreline with increasing bypass ratio. However the invariance against nozzle sizes is a fundamental finding and leads to the formulation of the second matching constraint. Moreover, it enhances the model to be applicable for industrial development processes, where nozzle size changes need to be represented accurately by performance synthesis calculations.

8. CONCLUSIONS

A physical approach for a steady-state model was introduced and discussed in this paper. The most relevant thermo- and gasdynamic effects could be pointed out and separated with this model. The advantages by using this approach could be proven by a clear breakdown of the detrimental and beneficial impacts of the exhaust system, hence this method gives clear indications of the improvement potential of an existing design. It could furthermore be demonstrated, that this model can be calibrated against rig- and engine test results with high fidelity. Thus it shows full capabilities for the usage in connection of full thermodynamic engine synthesis as well as analysis models. The newly introduced performance parameters are invariant against the operating condition of the exhaust system and hence indicate that the physical effects are well covered with the elementary flow models, which are discussed in this paper.

Besides, the discussed model dominates compared to conventional modelling approaches in various aspects. The strict two-stream approach keeps modelling uncertainties on lowest level as no back-to-back comparisons need to done. However, physical representation even supersedes the one of the three-stream model, where non-allocable effects are collected in the discharge- and thrust coefficient.

Those findings lead to the conclusion, that the physical exhaust model provides an enrichment of thermodynamic performance models with mixed nozzle configuration for existing turbofans as well as for models used in the design- or development project phase.

9. ACKNOWLEDGMENTS

The author wants to thank Rolls-Royce Deutschland Ltd. & Co KG for the support on the research work accomplished on this topic. Further thanks go to the Institut für Luftfahrtantriebe, Stuttgart for the fruitful discussions on that topic and explicitly to Joachim Schwing as well as Florian Wolters who contributed to the development on this paper.

10. REFERENCES

[1] T. Frost, 1966, “Practical Bypass Mixing Systems for Fan Jet Aero Engine”, Aeronautical Quarterly, **5**, pp. 141-160

[2] H. Pearson, 1962, “Mixing of exhaust and bypass flow in a bypass engine”, The journal of the royal aeronautical society, **66**, pp. 528-530

[3] A. Alexiou, K. Mathioudakis, 2005, “Development of Gas Turbine Performance Models using a generic Simulation Tool”, ASME Paper, GT2005-68678

[4] R. Köhli, S. Staudacher, H. Schulte, K. Schmidt, 2004, „Validierung eines Performancemodells für ein Turbofantriebwerk im tiefen Teillastbereich”, DGLR Paper, 2004-180

[5] J. Lieser, B. Deinert, C. Möller, F. Müller, 2007, “Numerical Simulation of mixed Jet Exhaust System and its Verification”, CEAS Paper, 2007-449

[6] A. Kuchar, R. Chamberlin, 1983, “Scale Model Performance Test Investigation of Mixed Flow Exhaust Systems for an Energy Efficient (E^3) Propulsion System”, AIAA-83-0541

[7] J. Wachter, F. Köpf, 2009, “Advanced Exhaust Performance Modelling of Mixed Turbofan Engines – Less is More”, ASME Turbo Expo 2009, GT2009-59947

[8] G. Oates, “Performance Estimation for Turbofans with and without mixers”, Journal of Propulsion, 1(**3**), pp. 252-256

[9] R. Dieck, 2007, “Measurement Uncertainty – Methods and Applications“, ISA

[10] U. Simon, 1969, „Das stationäre Betriebsverhalten von Zweikreis-Turbostrahltriebwerken mit Strahlmischung”, Dissertation Universität Stuttgart

[11] B. Banzhaf, S. Staudacher, 2007, „Experimentelle und numerische Untersuchungen zum Betriebsverhalten des Triebwerksmischers im niedrigen Lastbereich”, CEAS Paper, 2007-125

[12] C. Riegler, M. Bauer, H. Schulte, 2003, “Validation of a Mixed turbofan Performance Model in The Sub-Idle Operating Range”, ASME Turbo Expo 2003, GT2003-38223

[13] Schlichting, Gersten, 2006, „Grenzschicht-Theorie”, 10. Auflage, Springer-Verlag

[14] H. Baehr, S. Kabelac, 2006, „Thermodynamik“, 13. Auflage, Springer-Verlag